BB

KEK Preprint 96-158
January 1997
H

Scalar and Vector Meson Production and Two-Step Processes in (K^-, K^+) Reaction on ^{12}C

E224 Collaboration

Submitted to Nuclear Physics, A.

National Laboratory for High Energy Physics, 1997

KEK Reports are available from:

Technical Information & Library
National Laboratory for High Energy Physics
1-1 Oho, Tsukuba-shi
Ibaraki-ken, 305
JAPAN

Phone: 0298-64-5136
Telex: 3652-534 (Domestic)
(0)3652-534 (International)
Fax: 0298-64-4604
Cable: KEK OHO
E-mail: Library@kekvax.kek.jp
Internet: http://www.kek.jp

Scalar and Vector Meson Production and Two-Step Processes in (K^-, K^+) Reaction on ^{12}C

E224 Collaboration

J.K. Ahn[a], S. Aoki[d], K.S.Chung[k], M.S.Chung[j], H. En'yo[a], T.Fukuda[e], H. Funahashi[a], Y. Goto[a*], A. Higashi[e],M. Ieiri[f], T. Iijima[f], M. Iinuma[a], K. Imai[a], Y. Itow[a†], J.M. Lee[k], S. Makino[a],A. Masaike[a], Y. Matsuda[a], Y. Matsuyama[e], S. Mihara[a],C. Nagoshi[c], I. Nomura[h], I.S. Park[j], N.Saito[a*], M. Sekimoto[e], Y.M. Shin[i], K.S. Sim[j], R. Susukita[a*], R. Takashima[b], F. Takeutchi[c], P. Tlustý[e‡], S. Weibe[i], S. Yokkaichi[a], K. Yoshida[a], M. Yoshida[a*],T. Yoshida[g], S. Yamashita[a§]

[a] *Department of Physics, Kyoto University, Kitashirakawa-Oiwake, Kyoto 606, Japan*

[b] *Kyoto University of Education, Fukakusa-Fujinomori, Kyoto 612, Japan*

[c] *Kyoto Sangyo University, Kamigamo-Motoyama, Kyoto 606, Japan*

[d] *Faculty of Human Development, Kobe University, Nada, Kobe 657, Japan*

[e] *Institute for Nuclear Study, University of Tokyo, Tanashi, Tokyo 188, Japan*

[f] *KEK, National Laboratory for High Energy Physics, Oho, Tsukuba 305, Japan*

[g] *Department of Physics, Osaka City University, Sumiyoshi, Osaka 558, Japan*

[h] *National Institute for Fusion Science, Nagoya 464-01, Japan*

[i] *University of Saskatchewan, Saskatoon, Canada*

[j] *Department of Physics, Korea University, Seoul 136-701, Korea*

[k] *Department of Physics, Yonsei University, Seoul 120-749, Korea*

January 7, 1997

Abstract

The double strangeness exchange, (K^-, K^+), reaction has been investigated with a scintillating fiber active target at $p_{K^-} = 1.66$ GeV/c. The differential cross sections of the two step processes involving a pair of hyperons(Λ or Σ) and the subthreshold production of scalar and vector meson, $f_0/a_0/\phi$, in the (K^-, K^+) reaction on ^{12}C have been measured for $p_{K^+} = 0.6 - 1.3$ GeV/c. The differential cross sections($< d\sigma/d\Omega_L >$) of the $^{12}C(K^-, K^+)\Lambda\Lambda X$ and $^{12}C(K^-, K^+)\Lambda\Sigma X$ reactions are 17 ± 4 and 2.3 ± 1.0 μb/sr, respectively. The upper limit of that for the $^{12}C(K^-, K^+)\Sigma\Sigma X$ reaction has been obtained to be 0.17 μb/sr at 90 % confidence level. The differential cross section for the subthreshold scalar and vector meson production is 11 ± 6 μb/sr at $600 \leq p_{K^+} < 950$ MeV/c. These experimental results lead us to a conclusion that the two-step processes accompanying two hyperon states give a considerably larger contribution to the (K^-, K^+) reaction, while the subthreshold $f_0/a_0/\phi$ meson productions give much less contribution than the theoretical calculation by C.Gobbi, C.B.Dover, and A.Gal.

*present address: *RIKEN, Institute for Physical and Chemical Research, Wako, 351-01, Japan*

†present address: *Institute for Cosmic Ray Research, University of Tokyo, Tanashi, Tokyo 188, Japan*

‡present address: *Nuclear Physics Institute of the Academy of Science, 250 68 Řež, Czech Republic*

§present address:*International Center for Elmentary Particle Physics,University of Tokyo,Tokyo 113,Japan*

1 INTRODUCTION

The (K^-, K^+) reaction on nuclei has, recently, attracted much attention, since it was suggested to be an efficient channel to produce both the H dibaryon and double strangeness nuclei such as Ξ and $\Lambda\Lambda$ hypernuclei [1, 2, 3]. Several experiments have been carried out to search for the H dibaryon and the double strangeness nuclei through the (K^-, K^+) reactions at the incident K^- momenta from 1.65 to 1.8 GeV/c [4, 5, 6, 7, 8]. The H dibaryon was searched for by the (K^-, K^+) reactions on ^3He (BNL-E836)[4], nuclear emulsion (KEK-E176)[5], and a scintillating fiber active target (KEK-E224)[6]. The evidence of the H dibaryon was, so far, not observed by these experiments. On the other hand, the production of double Λ hypernuclei by the (K^-, K^+) reaction on the emulsion nuclei was reported as well as those produced following the stopping Ξ^- in the emulsion [9, 10]. In order to extend such studies, it is quite important to understand the mechanism of the (K^-, K^+) reaction on nuclei. The (K^-, K^+) reaction is also of considerable intrinsic interest in the field of nuclear reaction since it is a double charge and strangeness exchange reaction.

The elementary reactions such as $K^-p \rightarrow K^+\Xi^-$ and $K^-p \rightarrow K^+\Xi^{*-}$ were studied by many experiments with hydrogen bubble chambers long time ago [11]. The (K^-, K^+) reaction on nuclei was also observed with a heavy liquid bubble chamber at $p_{K^-} = 2.1$ GeV/c [12]. However, the statistics was too limited for the study of the reaction mechanism and the emphasis was laid on the resonance search in the $\Lambda\Lambda$ and Ξ^-p invariant mass spectra. Recently, Iijima et al. have measured the cross sections of (K^-, K^+) reactions on nuclear targets, C, Al, Cu, Ag and Pb, at $p_{K^-} = 1.65$ GeV/c as a function of the K^+ momentum [13]. For all the nuclear targets, the K^+ momentum spectrum was characterized by a peak at $p_{K^+} = 1.1$ GeV/c and a large bump in the low momentum region from 0.6 to 0.8 GeV/c, each corresponding kinematically to the quasifree Ξ^- and Ξ^{*-} productions, respectively. The cross section for the peak was well reproduced by the DWIA calculation for the quasifree Ξ^- production for all the nuclei. However, the cross section for the bump was a factor of $4 \sim 6$ larger than the DWIA calculation for the quasifree Ξ^{*-} production. It raised a puzzling question.

Iijima et al. proposed that the excess of the cross sections could be largely due to the contribution of two step processes such as the processes of $\pi N \rightarrow YK^+$ following the single strangeness exchange reaction, $K^-p \rightarrow \pi Y$, where Y denotes Λ or Σ. However, recently Gobbi et al. claimed against the dominance of two-step processes at low K^+ momenta, and suggested the scalar($f_0(975)$ and $a_0(980)$) and vector mesons($\phi(1020)$), were abundantly

produced in the first order process, $K^-p \to f_0\Lambda, a_0\Lambda$, and $\phi\Lambda$, subsequently followed in part by the K^-K^+ decay [14]. It must be noticed that the scalar and vector mesons are produced in the subthreshold energy and the internal nuclear momentum distribution is a crucial point in the evaluation of the cross sections. Moreover, no experimental result for the $K^-p \to \Lambda\phi$ reaction is available from the threshold momentum(1.76 GeV/c) to 1.95 GeV/c, and the $K^-p \to f_0\Lambda/a_0\Lambda$ reactions and the branching ratio of $a_0(980) \to K^-K^+$ are not clearly known so far.

More recently, a new theoretical calculation has been performed to investigate the (K^-, K^+) reactions on nuclear targets at $p_{K^-} = 1.65$ GeV/c. Based on the Intra-Nuclear-Cascade(INC) model, Nara et al. reproduced the K^+ momentum spectra [15]. The INC model calculation included all possible species of meson and hyperon families within the kinematically allowed regions for the two-step processes. The results of the INC model calculation showed the scalar and vector meson productions were roughly a factor of two smaller than the Gobbi et al.'s result.

We have carried out an experiment to observe the (K^-, K^+) reaction on a scintillating fiber(SCIFI) active target by using 1.66 GeV/c K^- beam. The primary motive of the experiment was to search for the H dibaryon through direct process, $K^-(pp) \to HK^+$ [16] and atomic capture process, $(\Xi^-, C)_{atom} \to HX$ [6]. At the same time, we could study the detail of the (K^-, K^+) reaction on carbon by using the visual information from the SCIFI target. The SCIFI target acts as both interaction target and track detector, and provides a photon image of charged particle tracks around the (K^-, K^+) reaction vertices. It has an advantage over a bubble chamber on the achievable statistics since it is a high rate and triggerable detector, and the data can be easily analyzed by a computer. Compared to the emulsion, the target composition is simple(CH) and the Λ production can be easily identified, which is essential to study the reaction channels with Λ production.

In this paper, we describe the results of the SCIFI data analysis of more than 2000 events for the (K^-, K^+) reaction in the wide range of K^+ momentum in order to study its reaction mechanism. We present the cross section of f_0, a_0 and ϕ meson productions in the subthreshold energy, as well as those of the two-step processes with respect to the final hyperon states, $^{12}C(K^-, K^+)\Lambda\Lambda X$, $^{12}C(K^-, K^+)\Lambda\Sigma^- X$, and $^{12}C(K^-, K^+)\Sigma^+\Sigma^- X$ reactions at $p_{K^-} = 1.66$ GeV/c. We discuss the Ξ^{*-} production off carbon nuclei as well.

2 EXPERIMENT

The experiment was carried out by using a separated K^- beam at the KEK proton synchrotron. The experimental setup is shown in Fig. 1. The typical K^-/π^- ratio of the beam was 1/4 at the intensity of $2 \times 10^4 K^-$/spill ($\sim$ 2 sec). The central momentum of the K^- beam was 1.66 GeV/c with a spread of 0.06 GeV/c(FWHM). The incident K^-'s were identified with an aerogel Cherenkov detector(BAC). Combined with the time-of-flight(TOF) information(T2$-$T1, Δt = 85 psec[rms]), the contamination of π^- and $\bar{p}$ was reduced to less than 0.01 %. The beam momentum was measured by using a 5 set of multiwire proportional chambers(BPC1-5) with the resolution of $\Delta P/P = 0.5\%$(rms) [18].

Identification of outgoing K^+'s was achieved by momentum and velocity measurements in the spectrometer. Particle trajectories, through a dipole magnet with the maximum field of 1.1 Tesla, were measured by 3 sets of drift chambers, DC1, DC2 and DC3. A hodoscope(CH) of 12 plastic scintillators was placed before the magnet and a TOF hodoscope(FTOF) composed of 24 plastic scintillators was located 5 m downstream the SCIFI target. Time-of-flight was measured with the FTOF hodoscope and the T2 scintillation counter, and overall time resolution of the TOF measurement was 110 psec(rms). The vertical hodoscope(YH) of 6 plastic scintillators defined the geometrical acceptance of the spectrometer, which was about 0.09 sr. The lucite(LC) and aerogel Cherenkov(SAC) detectors discriminated kaons from protons and π's. The refractive indices for LC and SAC were 1.59 and 1.04, respectively.

The SCIFI target was made of scintillating fibers of 0.5mm square shape. It contained almost equal amounts of carbon and hydrogen atoms. As shown in Fig. 2, 200 flat sheets, each made with 160 plastic fibers, were stacked to form a $8 \times 8 \times 10cm^3$ block. Each fiber sheet was laid alternately in X and Y directions, i.e., transverse to the beam direction(Z). The SCIFI target was viewed by two sets of the image intensifier tube(IIT), which were arranged orthogonally(X and Y). The spacing between adjacent fiber sheets out of the target volume was reduced to match the $8 \times 10cm^2$ target area(XZ and YZ) of each direction to the effective photo-sensitive area($8cm\phi$) of the IIT. Black acryl plates of 300μm thick were inserted between the fiber sheets out of the target volume to prevent cross talks. Each set of IIT(Delft PP0040) had a cascade structure of three individual IIT's. The second and third stage IIT's were triggerable. An intensified photon image was viewed with a CCD camera, and was digitized by a flash ADC. The average number of detected photons for a minimum ionizing particle was about 0.55/mm along the track for each direction, and the position resolution was about 290 μm [19]. The SCIFI target was surrounded by a cylindrical drift

chamber(CDC) and TOF counters(BTOF) to detect particles coming out of the SCIFI target. The details of this detector will be reported elsewhere [20].

Due to the read-out frequency of the CCD(30 Hz), a fast and efficient method was needed to reduce the trigger rate to a manageable level, about 20 events/spill. To accomplish this, the trigger system was divided into two stages. The first level trigger selected positively charged particles passing through the YH, which were discriminated from π's and protons by Cherenkov counters(SAC and LC). The coincidence of hit information between FTOF and CH enabled us to determine the electric charge of outgoing particles as fast as to hold the image within 2.4 μs decay time of the phosphor of the first stage IIT's. The second level trigger was made by fast electronics to calculate the masses of the scattered particles within 15 μs, using TOF information obtained by a fast encoding TDC system(Lecroy TAC + FERA ADC) and momenta determined by hit positions on the FTOF and the CH. The first level trigger signal gated the second stage IIT's, while the second level trigger signal was applied to the last stage of IIT's. The trigger efficiency for scattered K^+ was 93%. The total dead-time of the online data-taking was 20%.

3 DATA ANALYSIS

The tagged K^+ particles were again selectively discriminated from π^+'s and protons by off-line analysis. The momenta of particles were reconstructed from hit information on drift chambers by means of the Runge-Kutta method. The momentum resolution ($\Delta P/P$) was 0.5% (rms) at 1.2 GeV/c [6]. The K^+ momentum and the missing mass spectra are shown in Fig.3. The proton target was assumed for the calculation of missing mass. Both spectra were obtained by selecting K^+ particles whose reconstructed mass ranges from 440 MeV/c^2 to 550 MeV/c^2. The background ratio of π^+ and proton to K^+ was estimated to be less than 2 %, assuming the constant background.

Totally 3147 events were eye-scanned to investigate the mechanisms of the (K^-, K^+) reactions. The scanning volume was geometrically limited to the effective target volume viewed by the IIT-CCD read-out system. The fiducial volume for the interaction point along the beam direction(Z_{vtx}) was more tightly defined to make a reliable event selection. It covered the region of $-50mm \leq Z_{vtx} \leq +36mm$ at the center of the SCIFI target. Out of 3147 events, 2148 events were identified as the interaction events within the fiducial volume.

The number of events at high K^+ momenta ($p_{K^+} \geq 950$ MeV/c) was 1355, while that at low K^+ momenta was 793. We categorized all of 2148 interaction events with respect

to their event topologies, such as numbers of charged prongs, kinks and Λ's. They were globally divided into 5 groups, D, Y, I, K, and X-types. The schematic drawings of the event topologies are shown in Fig. 4.

Both D and Y-types have their subsets of DV and YV-type, respectively, concerning visible Λ decays. The DV-type is defined as the event topology in which Ξ^-(or others) decays into Λ and π^-, and the Λ decays visibly. If the Λ comes from a kink point, the DV-type event was further studied for the $\Xi^* \rightarrow \Xi^-\pi^0$ channel at low K^+ momenta. However, if the Λ decay point is not matched to the kink point but to the K^- interaction vertex, the Λ should be independently produced via a multi-step process. The D-type is the parent set of the DV-type, and also contains the events of which Λ decay is missing (Λ escapes or decays into neutrals). The definition of Y- and YV-types is in the similar manner. The Y-type has only one additional prong which looks consistent with the $\pi^\pm$ or K^-'s track, while the YV-type is, in particular, the Y-type with a visible Λ decay. The I-type stands for the interaction of the Ξ^- particle. One charged prong comes out of the primary vertex, and stops within the scanning volume. It contains, however, the stopping protons which probably come from the nuclear evaporation of the ^{12}C, as well as the stopping Ξ^-'s. The K-type has no additional prong at the vertex. The Ξ nuclear absorption and the emission of neutral particles are plausible in the K-type. Finally, the X-type includes all the multi-prong(more than 2 prongs other than K^+ track) events which are largely due to the multi-step process inside carbon nuclei.

The computerized eye-scanning system has minimized the error of a human-dependent pattern recognition. The (K^-, K^+) event selection was assisted by chamber data. The chamber data were graphically guided to filter ghost tracks which were not associated with the (K^-, K^+) reaction. Moreover, comparison between two projection views(XZ and YZ) enabled us most reliably to determine the positions of the interaction, decay, and stop points. Since the event topology was categorized simply with respect to numbers of charged prongs, kinks and Λ's, present analysis was not much sensitive to the human-dependent categorization. One-tenth of total data were doubly eye-scanned independently. The error of the human-dependent categorization was less than 6 %, and the difference of the position measurements for the K^- interaction vertex was 1 mm(rms) in the beam direction(Z). The error of the categorization was mainly due to the human dependence on identifying short tracks, which was corrected by the scanning efficiency in terms of the track length. The results of the categorization are shown in Table 1.

Table 1: Event topology of (K^-, K^+) reactions

Topology	D (DV)	Y (YV)	I	K	X	Total
# of events(all)	787 (281)	479 (97)	316	293	273	2148
# of events						
($p_{K^+} \leq 950$ MeV/c)	154 (35)	241 (62)	89	100	199	793

3.1 Y-Type

The $K^- p \rightarrow f_0\Lambda, a_0\Lambda$, and $\phi\Lambda$ process belongs topologically to the Y-type. The particle tracks of the K^- beam and the $f_0/a_0/\phi \rightarrow K^- K^+$ decay makes the Y-type event topology. If the $f_0/a_0/\phi$ meson productions are predominantly ample at low K^+ momenta, their $K^- K^+$ decay topologies should be observed in the photon images of the SCIFI target, despite of the narrow experimental acceptance plunging to zero below $p_{K^+} = 500$ MeV/c. When a Λ decays visibly, the topology of the f_0, a_0, and ϕ meson productions is ambiguous only with the quasifree Ξ^* production, where the Ξ^* resonance decays via $\Xi^* \rightarrow \Xi^0\pi^-$, followed by $\Xi^0 \rightarrow \Lambda\pi^0$. The other decay mode, $\Xi^-\pi^0$, resembles mostly the topology of the D-type, while a small portion of this mode involving a short Ξ^- hyperon may fall into the category, Y-type.

These backgrounds due to the Ξ^0 and the short Ξ^- can be supressed by requiring a visible Λ decay. Since the average flight length of the Ξ^0 hyperon is 3.5 cm long ($c\tau_{\Xi^0} \simeq 8.71$ cm) in the SCIFI target, the probability of a visible Λ decay ($c\tau_\Lambda \simeq 7.89$ cm) from the Ξ^0 becomes small. Moreover, the backgrounds due to the Ξ^0 and the short Ξ^- are more efficiently suppressed by the additional criterion on the Λ decay, such that the decay proton should be stopped within the scanning volume. This is because Λ momentum for the $f_0/a_0/\phi$ production is rather higher than that for the backgrounds. In addition, the flight length of Λ for the $f_0/a_0/\phi$ production is potentially longer than that for the backgrounds, since the origin of Λ is different.

The Λ masses were reconstructed from the decay angles of proton and π^-, and the range of proton. The kinetic energy of the stopping proton was deduced from the empirical formula (inferred from the experimental data [19]). To insure that none of e^+e^- pair is mis-identified for the Λ, we excluded the events if the tracks are curled in a scanning volume. The curled tracks are attributed to the e^-e^+ pair production from low energy gamma ray under a fringe field of about 30 gauss. Energetic e^+e^- pairs should escape from the scanning volume, which

could be originated from the π^0 decay. Since we selected the Λ which decayed into p and π^- with the proton stopping inside the scanning volume, those energetic e^-e^+ pairs were excluded.

The following selection criteria have been applied to select the $K^-p \to f_0\Lambda, a_0\Lambda$ and $\phi\Lambda$ reactions followed by $f_0/a_0/\phi \to K^-K^+$ decays.

1. Events were required to have exactly a visible Λ decay of which a decay proton should be stopped inside the scanning volume.

2. Missing mass should be larger than 1450 MeV/c^2 to diminish the contributions of other processes more effectively.

3. An opening angle between K^+ and the other charged prong at the primary vertex should be less than 30^o.

4. Reconstructed Λ mass with the primary vertex should be located within the tolerance window of $\mid m_\Lambda - 1115.7\ (\mathrm{MeV}/c^2) \mid \ \leq 60\ (\mathrm{MeV}/c^2)/L_\Lambda$, where L_Λ is the flight length of Λ in mm, and the mass tolerance, 60 MeV/c^2, accounts for the systematic error due to the angular resolution, $\delta\theta = 500/R_p$ (mrad) depending on the range of the stopping proton (R_p in mm).

The rationale behind this opening angle selection is that the OZI allowed decay $\phi \to \bar{K}K$ has very little phase-space available since the ϕ mass (1020 MeV/c^2) is barely above $\bar{K}K$ threshold. Hence, the K^+K^- pair are Lorentz-boosted towards the forward angles. Monte Carlo study indicates that the opening angles of the K^-K^+ pairs lie below 30^0. After imposing these selection criteria, 6 events remained at $600 \leq p_{K^+} < 950$ MeV/c. A typical SCIFI image of the $f_0/a_0/\phi$ meson productions is shown in Fig.5

3.2 D-type

The D-type events are largely populated at the Ξ^- production region, while they are uniformly distributed at low K^+ momenta. Below the Ξ^- production peak, the D-type events have the two first- order processes. One is the $K^-p \to \Xi^-K^+$ off a bound nucleon inside a carbon nucleus, and the other is the $K^-p \to \Xi^{*-}K^+$, followed by $\Xi^{*-} \to \Xi^-\pi^0$. There is also a contribution of the two step process such as $K^-p \to \pi^+\Sigma^-; \pi^+n \to K^+\Lambda$. To resolve the contribution of the $K^-p \to \Xi^{*-}K^+$, followed by $\Xi^{*-} \to \Xi^-\pi^0$, all DV-type events at low K^+ momenta were investigated with a similar selection criteria to the $f_0/a_0/\phi$

production event (condition (1) and (4)). Instead of the opening angle criterion, the coplanar condition on Ξ^- decay plane was imposed to reconstruct the Ξ^-. The coplanarity angle, ψ is defined as $\psi = 90^o - \cos^{-1}(\vec{k}_\Xi \times \vec{k}_\pi \cdot \vec{k}_\Lambda)$, and should be less than 30^o. In addition, the reconstructed Ξ^- momenta should be larger than 300 MeV/c.

Out of 35 DV-type events, 14 events were identified as DV-type(stopping p) such that the Λ decayed into p and π^-, and the decay proton was stopped in the scanning volume. After imposing the above selection criteria, 7 events remained as candidate events for the process, $K^-p \to \Xi^{*-}K^+$, followed by $\Xi^{*-} \to \Xi^-\pi^0$. The other 7 events were in favor of the two-step process hypothesis since the reconstructed Λ masses were better matched with the primary interaction points than with the Ξ^- decay vertices. Those events turned out to be $^{12}C(K^-, K^+)\Lambda\Sigma^- X$.

3.3 Two Λ Events

Analysis of events having two Λ's plays a decisive role to figure out what kind of processes causes to make broad bump at low K^+ momenta. Two Λ's can be produced via the following two-step processes,

$$K^-N \to \begin{pmatrix} \pi \\ \eta \\ \rho \\ \omega \\ \eta' \end{pmatrix} \begin{pmatrix} \Lambda \\ \Sigma^0 \\ \Sigma^* \end{pmatrix} \quad ; \quad \begin{pmatrix} \pi \\ \eta \\ \rho \\ \omega \\ \eta' \end{pmatrix} N \to K^+ \begin{pmatrix} \Lambda \\ \Sigma^0 \\ \Sigma^* \end{pmatrix}$$

$$K^-p \to K^+\Xi^- \quad ; \quad \Xi^-p \to \Lambda\Lambda, \ \Sigma^0\Lambda.$$

The two Λ events were further categorized in Table 2, with respect to the number of additional charged prongs at the primary vertices. The minimum length and opening angle of decay particles were imposed to make a reliable selection of the Λ. Both decay particles should leave their tracks longer than 2(mm), and the opening angle should be larger than $3 \cdot \delta\theta$, where $\delta\theta$ is 500(mrad)/L(mm), and L is the flight length of the decay particle. A typical $\Lambda\Lambda$ production event is shown in Fig. 6.

No additional prong indicates that both Λ's came from the two-step processes accompanied with Λ or Σ^0 production in the first and second processes. Two events containing a single escape prong can be understood to produce π via a Σ^* hyperon in either first or second

Table 2: Number of charged prongs in 2 Λ events.

# of prongs(event topology)	0(K)	1-stop(I)	1-escape(Y)	$\geq$ 2(X)	Total
# of events (all)	14	11	2	1	28
# of events ($p_{K^+} < 950$ MeV/c)	7	7	2	1	17

process. Rest of them carried one or more charged baryons, and are mainly due to nuclear evaporation of residual nuclei during the two-step process.

4 RESULTS AND DISCUSSIONS

The Monte Carlo method was utilized to reproduce the productions of the $f_0/a_0/\phi$ meson and the Ξ^* hyperon, which are followed by the subsequent decays, and the two step process producing two hyperons ($S = -1$). The beam was initially produced at the central momentum of 1.66 GeV/c, and was spread with the *rms* resolution of 21 MeV/c. The Monte Carlo simulation procedure included the detection efficiency of the K^+ online with respect to the K^+ momentum, and the efficiency of the SCIFI target. The low momentum K^+'s were largely suppressed by the online trigger. Since the E224 spectrometer and trigger system were designed to tag the high momentum K^+ particles which were accompanied with low energy Ξ^-'s. Therefore, two third of 700 MeV/c particles and one fifth of 600 MeV/c particles were triggered, while high momentum particles over 800 MeV/c were most effectively accepted. The Monte Carlo simulation reproduces the momentum dependence of the experimental acceptance for K^+ particles with 5 % error on average at $600 \leq p_{K^+} < 800$ MeV/c ($\sim$ 1% error at $800 \leq p_{K^+} \leq 1300$ MeV/c).

In the target region, the geometrical fiducial volume is defined as the net volume made by the geometry of the target and the IIT window, since the IIT window did not cover the whole area of the target. In addition, the effective scanning volume was included to prevent from the ambiguity of event selection near the boundary of the geometrical fiducial volume. Due to the finite resolution of the SCIFI target, a very short track could not be resolved systematically. All the systematic factors scaling down the detection efficiency were included in the procedure of Monte Carlo simulation. To prove the reliability of the simulation, the response function of the SCIFI detector was examined for the $K^-p \rightarrow K^+\Xi^-$, followed by $\Xi^- \rightarrow \Lambda\pi^-$. The ratio of the number of visible Λ decays to the total number of the quasifree

Ξ^- productions is sensitive to both the geometry of the SCIFI target and scanning efficiency. The Monte Carlo simulation reproduced that 38% Λ's decayed visibly inside the scanning volume, being well consistent with the experimental data (39 ± 3 %).

The production cross section was evaluated by using the absolute cross section data of the previous experiment [13]. The angular distribution for the $K^-p \rightarrow K^+\Xi^-$ reaction was inferred from the old data of the hydrogen bubble chamber experiment [11]. The differential cross section averaged over an angular interval, is given by

$$\langle \frac{d\sigma}{d\Omega_L} \rangle = \int_{\cos\theta_{min}}^{\cos\theta_{max}} \frac{d\sigma}{d\Omega_L} \; d(\cos\theta) \; / \int_{\cos\theta_{min}}^{\cos\theta_{max}} d(\cos\theta) \qquad (1)$$

where θ_{min} is 2.3^o and θ_{max} is 14.7^o. The differential cross section averaged over the above angular interval, $\langle \frac{d\sigma}{d\Omega_L} \rangle^{SCIFI}_{K^-p \rightarrow K^+\Xi^-}$, was deduced from the product of the effective proton number of the SCIFI target and the differential cross section averaged over the angular acceptance ($\langle \frac{d\sigma}{d\Omega_L} \rangle^{H}_{K^-p \rightarrow K^+\Xi^-} \cdot (1 + Z^{\Xi^-}_{eff}) = 116 \pm 13$ μb/sr, where $Z^{\Xi^-}_{eff} = 2.36$) [13, 22]. The differential cross section averaged over the angular interval is given by

$$\langle \frac{d\sigma}{d\Omega_L} \rangle^{SCIFI} = N_0 \frac{Y}{\eta_{SFD} \cdot \eta(p_{K^+}, \theta_{K^+})_{SP} \cdot \eta_{K^+dec}}, \qquad (2)$$

where Y is the experimental yield, and η_{SFD} is the detection efficiency in the SCIFI target. The $\eta(p_{K^+}, \theta_{K^+})_{SP}$ indicates the experimental acceptance of the spectrometer, and η_{K^+dec} accounts for the survival rate of the scattered K^+ particle traveling up to the FTOF counter placed 5 m away from the target center. N_0 is the normalization factor, which is given by

$$N_0 = \langle \frac{d\sigma}{d\Omega_L} \rangle^{SCIFI}_{K^-p \rightarrow K^+\Xi^-} \frac{\eta(p_{K^+}, \theta_{K^+})^{\Xi^-}_{SP} \cdot \eta^{\Xi^-}_{K^+dec}}{N^{(p \geq 950MeV/c)}_{(K^-,K^+)} \cdot R_{\Xi^-} / \eta^{(p \geq 950MeV/c)}_{\Xi^-}} \qquad (3)$$

Here, $N^{(p \geq 950MeV/c)}_{(K^-,K^+)}$, is the experimental yield of (K^-, K^+) reaction above $p_{K^+} = 950$ MeV/c in the SCIFI target. The ratio of the Ξ^- production to the (K^-, K^+) reactions, R_{Ξ^-}, was 0.81 ± 0.033 at high K^+ momenta (950 MeV/$c \leq p_{K^+} \leq$ 1300 MeV/c) [23]. The factor, $\eta^{(p \geq 950MeV/c)}_{\Xi^-}$, represents the probability that K^+ momenta of the $K^-p \rightarrow K^+\Xi^-$ reaction lie above 950 MeV/c, and it was estimated to be 0.90.

4.1 Scalar and vector meson production

Despite of detecting all the charged final states, the $f_0/a_0/\phi$ mesons could not be reconstructed event by event, since all of them were produced off the bound protons moving inside carbon nuclei. Much attention to the estimation of the detection efficiency and backgrounds was paid to obtain the cross section of the scalar and vector meson production. The

differential cross section of the $f_0/a_0/\phi$ meson production was calculated as follows,

$$\langle \frac{d\sigma}{d\Omega_L} \rangle^{SCIFI}_{\Lambda(M\to K^-K^+)} = N_0 \frac{Y_{\Lambda(\text{stopping p})M(\to K^-K^+)}}{\eta_{SFD} \cdot \eta(p_{K^+}, \theta_{K^+})_{SP} \cdot \eta_{K^+dec}}, \quad (4)$$

where M denotes the f_0, a_0 and ϕ mesons. The experimental yield, $Y_{\Lambda(\text{stopping p})M(\to K^-K^+)}$, is the number of events, where the Λ decays visibly and a decayed proton stops within the scanning volume, and the $f_0/a_0/\phi$ mesons decay into K^-K^+. The η_{SFD} accounts for the scanning efficiency in finding a visible Λ decay with a stopping proton. The η_{SFD} was estimated to be 11.5 % by the Monte Carlo simulation. In identifying Λ decay, the same selection criteria on the range of stopping proton and the opening angle between p and π^- decay particles were imposed as described in **3.3**. The branching ratio of $\Lambda \to p\pi^-$ (0.639) was included in the η_{SFD} [24]. Under the selection criteria described in **3.1**, the background due to $K^-p \to \Xi^0\pi^-K^+$ via the quasifree $\Xi^*(1535)$ resonance were estimated to be about 15 % by the Monte Carlo simulation. Other processes carrying a invisibly short Ξ^- decay became negligible after imposing the missing mass criterion.

The double differential cross section of the $f_0/a_0/\phi$ meson production with subsequent decay to K^-K^+ pair is shown in Fig. 7. The solid line in the figure shows the result of the INC model calculation, whereas the dotted line the prediction by Gobbi et al. The present result is consistent with the INC model calculation, while is largely different from the prediction by Gobbi et al. The differential cross section is given by

$$\langle \frac{d\sigma}{d\Omega_L} \rangle_{\Lambda(f_0/a_0/\phi\to K^-K^+)} = 11 \pm 6\ \mu b/sr$$

,which is averaged over the angular interval, ($2.3^o \leq \theta^L_{K^+} \leq 14.7^o$) and integrated over the momentum region ($600 \leq p_{K^+} < 950$ MeV/c). The result is consistent with the INC model calculation, that is about 6μb/sr. The small discrepancy may be attributed to the $K^-p \to f_0\Sigma^0, a_0\Sigma^0$ and $\phi\Sigma^0$ productions as well as the lack of experimental data on the $f_0/a_0/\phi$ meson productions near the threshold energies and the decay branching ratios of those mesons($\to K^-K^+$). However, the differential cross section of Gobbi et al.'s calculation at $600 \leq p_{K^+} < 950$ MeV/c is $\sim 80\mu$b/sr, which is an order of magnitude larger than the present experimental data. As outlined in the introduction, the internal nuclear momentum distribution is a crucial point in the evaluation of the subthreshold productions of scalar and vector mesons. Gobbi et al. utilized 'effective incident momentum' to evaluate the effect of Fermi motion, and the threshold momentum is brought to be 1.1 GeV/c. Nara et al. claimed that this method gives a wrong kinematics and overestimates the cross sections of the scalar and vector mesons [15].

4.2 Two-step processes

The production cross sections of the two-step processes involving two $S = -1$ hyperons in the final state, $^{12}C(K^-, K^+)YYX$, where Y denotes Λ or $\Sigma^{\pm}$, were estimated as follows. The double differential cross sections with respect to the final states of hyperons are shown in Fig. 8. The dotted line shows the INC model calculation for the total contribution of the two-step processes [15].

The $^{12}C(K^-, K^+)\Lambda\Lambda X$ reaction was characterized as two visible Λ decays inside the scanning volume. The detection efficiency of two Λ decay in the SCIFI target, $\eta^{\Lambda\Lambda}_{SFD}$, is given by $Br^2(\Lambda \rightarrow p\pi^-) \cdot \eta_{\Lambda\Lambda}$. The scanning efficiency, $\eta_{\Lambda\Lambda}$, was deduced from the Monte Carlo simulation based on the real data to reproduce the scanning inefficiency due to the effect of the finite size of the SCIFI detector and short decays of the Λ's. The corrected number of events for the $^{12}C(K^-, K^+)\Lambda\Lambda X$ reaction is $28/\eta^{\Lambda\Lambda}_{SFD} = 141 \pm 27$. The differential cross section is estimated to be

$$\langle \frac{d\sigma}{d\Omega_L} \rangle_{^{12}C(K^-,K^+)\Lambda\Lambda X} = 17 \pm 3.6\ \mu b/sr,$$

which is integrated over $600 \leq p_{K^+} \leq 1300 MeV/c$. This reaction includes Σ^0 and Σ^* productions, followed by the $\Lambda\gamma$ and $\Lambda\pi^0$ decays, respectively. This cross section is quite larger than that of the previous DWIA calculation [13], which included only π as an intermediate meson. Hence, it accounts for the contributions of the $\{\Sigma^0, \Sigma^*\}$ and other intermediate mesons $\{\eta, \omega, \rho, \eta'\}$, as well as those of Λ and π [15].

The $^{12}C(K^-, K^+)\Lambda\Sigma^- X$ reaction was characterized as a visible Λ decay and a kink prong. The efficiency of the SCIFI target, $\eta^{\Lambda\Sigma^-}_{SFD}$, is given by the product of η_{Σ^-} and $\eta_\Lambda \cdot Br(\Lambda \rightarrow p\pi^-)$. The scanning efficiency for the Σ can not be calculated with the Monte Carlo simulation because the momentum of Σ can not be uniquely determined in the present experiment. The efficiency η_{Σ^-} was assumed to be similar to η_{Ξ^-}, since the lifetime of the $\Sigma^-(c\tau = 4.434cm)$ is comparable with that of the $\Xi^-(c\tau = 4.91cm)$. The number of events being in favor of the $^{12}C(K^-, K^+)\Lambda\Sigma^- X$ hypothesis is found to be 7. It is corrected to be 18 ± 7 after the efficiency correction. The differential cross section of the $^{12}C(K^-, K^+)\Lambda\Sigma^- X$ is estimated to be

$$\langle \frac{d\sigma}{d\Omega_L} \rangle_{^{12}C(K^-,K^+)\Lambda\Sigma^- X} = 2.3 \pm 1.0\ \mu b/sr$$

As for the $^{12}C(K^-, K^+)\Sigma^+\Sigma^- X$ reaction, only one event ($p_{K^+} = 880$ MeV/c) was clearly identified by two kink tracks from the interaction vertex. The upper limit for the integrated

cross section of the $^{12}C(K^-,K^+)\Sigma^+\Sigma^-X$ reaction was estimated by

$$\langle\frac{d\sigma}{d\Omega_L}\rangle^{^{12}C(K^-,K^+)\Sigma\Sigma X} \leq N_0\frac{3.89}{\eta^{\Sigma\Sigma}_{SFD}\cdot\eta_{SP}\cdot\eta_{K^+dec}} \quad \text{at 90 \% C.L.}$$

Since the $\Sigma^\pm$ always decay visibly, the detection efficiency ,$\eta^{\Sigma\Sigma}_{SFD}$,for $^{12}C(K^-,K^+)\Sigma^+\Sigma^-X$ reaction is larger than the above two reactions, and it was estimated to be 0.64 by the Monte Carlo simulation, assuming p_Σ = 500 MeV/c. The upper limit for this reaction was then estimated to be 0.17μb/sr at 90 % confidence level.

While the differential cross section of the $^{12}C(K^-,K^+)\Sigma^+\Sigma^-X$ reaction is relatively consistent with the DWIA calculation, those of the two-step reactions involving the Λ('s) are very large. This accounts for the role of the hyperon resonance states. Since the final state of the Λ in the Y^* decay mode is dominant, the $NN(K^-,K^+)Y^{(*)}Y^*$ reactions contributes to a sizable enhancement of the $^{12}C(K^-,K^+)\Lambda\Lambda X$ reactions. The INC model calculation includes the production and decay of these hyperon resonance states. The experimental data with respect to the final hyperon states are consistent with the INC result at low K^+ momenta. However, at the Ξ^- production region, the $\Lambda\Lambda$ final states were observed more than the INC model prediction. A possible mechanism for two Λ production is the $\Xi^-p \rightarrow \Lambda\Lambda$ conversion process inside carbon nuclei. The present result suggests the cross section of the $\Xi^-p \rightarrow \Lambda\Lambda$ reaction is large compared with that in the INC model calculation ($\sigma_{\Xi^-p\rightarrow\Lambda\Lambda} \simeq$ 2 mb at $p_{\Xi^-} \simeq$ 500 MeV/c).

4.3 Quasifree Ξ^* production

Since the Ξ^{*-} decays totally into the $\Xi\pi$ state, the quasifree Ξ^{*-} production belongs to either D or Y-type assuming no Ξ^*N interaction inside carbon nuclei. To resolve the Ξ^* productions out of the (K^-,K^+) reactions at low K^+ momenta, all the known background events were subtracted from the D and Y-type events. They are the quasifree Ξ^- production, $f_0/a_0/\phi$ meson production and the two-step processes, as described in the previous sections. The double differential cross section of the Ξ^* production followed by $\Xi^* \rightarrow \Xi\pi$ on the SCIFI target is shown in Fig.9. The integrated cross section is 67 ± 8 μb/sr, which is two-third as large as the Relativistic Impulse Approximation(RIA) result (~ 95 μb/sr)[15]. For carbon nuclei, the experimental result is a factor of two smaller than the RIA result. However, it should be noted that the D and Y-type contain the Ξ^* productions only when the Ξ^* decays into the $\Xi\pi$ state without emitting the charged tracks longer than 2 (mm). Since the RIA calculation does not include the Ξ^{*-} interactions inside carbon nuclei, Ξ^*N interactions in

^{12}C could be a possible explanation on the difference. However, the strengths of the Y^*N interaction have not been known to date.

The observed cross section for (K^-, K^+) reaction on the SCIFI target is 170 ± 7 μb/sr at $600 \leq p_{K^+} < 950$ MeV/c of which only two-third is attributed to the scalar and vector meson productions, the two-step processes and quasifree Ξ^-/Ξ^* productions, as described in this section. The remaining cross section in this momentum region is of order of 60 μb/sr, as shown in Fig.10. The multi-prong events are dominant(39 ± 4 μb/sr), while the no prong and 1-stop prong events are scarce in the Ξ^* production region. The multi-prong events can fill the gap between the RIA result and the experimental data on Ξ^* production, followed by $\Xi^* \rightarrow \Xi\pi$. However, the cross section of the elementary process, $K^-p \rightarrow \Xi^{*-}K^+$, used in the RIA calculation is inferred from the very poor statistics and inconsistency between the data of old bubble chamber experiments [21].

The multi-prongs from the (K^-, K^+) reaction vertex could be due to the secondary interaction of hyperons in nuclei, including the production and decay of hyperfragments. The probability of observing single hyperfragment was reported in the hybrid emulsion experiment (KEK-E176), which is about $4 - 6\%$ at $p_{K^+} \simeq 600 - 900$ MeV/c [25]. It corresponds to the cross section of order of a few μb/sr for the production and decay of single hyperfragments in (K^-, K^+) reaction on ^{12}C. Out of the multi-prong events, 23 % of the events are found to have a $\Lambda \rightarrow p\pi^-$ decay by eye-scanning, which corresponds to a half of the multi-prong events after correction of the detection efficiency.

5 CONCLUSION

The (K^-, K^+) reaction on the scintillating fiber(SCIFI) active target at $p_{K^+} = 1.66$ GeV/c has been measured to study the reaction mechanism. The (K^-, K^+) reaction was identified with the K^+ spectrometer system covering $\theta_L = 2.3^0$ to 14.7^0 angular range. The SCIFI target with $8 \times 8 \times 10cm^3$ effective volume allowed us to study the reaction vertex for each event to make further specification of each reaction. We have analyzed 2148 (K^-, K^+) reaction events of which interaction vertices are located within an appropriate fiducial volume. The events were categorized by the topology of charged particle tracks. By using the topological information and kinematical constraints, we have identified the events for several reaction processes and obtained the differential cross section for each process.

The differential cross section for the subthreshold scalar(f_0 and a_0) and vector(ϕ) meson production from ^{12}C followed by the K^-K^+ decay was 11 ± 6 μb/sr at $600 \leq p_{K^+} < 950$

MeV/c. The present result is consistent with the INC model calculation, while it is largely different from Gobbi et al.'s calculation. The reason of the overestimation by Gobbi et al. could be their method of the approximation about the nucleon Fermi motion, since the subthreshold production is quite sensitive to the nucleon momentum distribution.

The differential cross sections for the $^{12}C(K^-, K^+)\Lambda\Lambda X$ and $^{12}C(K^-, K^+)\Lambda\Sigma^- X$ reactions are 17 ± 4 and 2.3 ± 1.0 μb/sr for $p_{K^+} \geq 600$ MeV/c, respectively. The upper limit of that for $^{12}C(K^-, K^+)\Sigma^-\Sigma^+ X$ reaction is 0.17 μb/sr at 90 % confidence level. The two-step processes accompanying two $S = -1$ hyperons were proved to be sizable in the (K^-, K^+) reaction. Comparing with the DWIA calculation, the present result for $\Lambda\Lambda$ production indicates a large contribution from Σ^0,Σ^*, and intermediate heavy mesons ($\eta, \omega, \rho, \eta'$). The experimental values for the $^{12}C(K^-, K^+)\Lambda\Lambda X$ plus $^{12}C(K^-, K^+)\Lambda\Sigma^- X$ are rather close to the INC model calculation for the sum of all the two-step processes, $^{12}C(K^-, K^+)Y^{(*)}Y^{(*)}X$, where Y indicates Λ or Σ. An observed enhancement of the cross section for the $\Lambda\Lambda$ production compared to the INC model at around $p_{K^+} = 1.1$ GeV/c could be due to the $\Xi^- p \rightarrow \Lambda\Lambda$ reaction inside carbon nuclei. If this is the case, the $\Lambda\Lambda$ resonance search can be done in the $\Lambda\Lambda$ mass spectrum from the (K^-, K^+) reaction at the appropriate K^+ momentum region.

The Ξ^* production cross section was estimated to be 67 ± 8 μb/sr. It is only two third as large as the result of the RIA calculation. Since the RIA calculation does not include the Ξ^* interactions in nuclei, Ξ^*N interactions in nuclei could be a possible explanation on the difference. However, the cross section of the elementary process, $K^- p \rightarrow \Xi^{*-} K^+$, used in the RIA calculation is inferred from the very poor statistics of old bubble chamber experiments and inconsistency between the data. In order to make a reliable and quantitative discussion on the Ξ^*N interactions in nuclei, one needs the data of the elementary process with much better precision.

We have observed many events which have multi-prongs from the reaction vertex. They are due to the secondary interaction of hyperons and include the production and decay of hyperfragments. Further study is necessary to understand these events.

ACKNOWLEDGEMENTS

We would like to thank the staff of the KEK proton synchrotron for their continuous support. We also thank Professor Y. Akaishi and Dr. Y. Nara for valuable discussions. This work was supported in part by the Basic Science Research Institute Program(BSRI-95-2408), the Ministry of Education, Korea, and a Grant-in-Aid for Scientific Research(02402008), the Ministry of Science, Culture and Education, Japan.

References

[1] A.T.M. Aerts and C.B. Dover, Phys. Rev. D28 (1983) 450.

[2] C.B. Dover and A. Gal, Ann. Phys. 146 (1983) 309.

[3] A.J.Baltz, C.B. Dover and D.J. Millener, Phys. Lett. B123 (1983) 9.

[4] R.W. Stotzer et al., to be published in Phys. Rev. Lett.

[5] S. Aoki et. al., Phys. Rev. Lett. 85, (1990) 1729.

[6] J.K. Ahn et. al., Phys. Lett. B378, (1996) 53.

[7] P.D. Barnes, Nucl. Phys. A547,(1992) 3c.

[8] M. May and G. Franklin, BNL-E885 looked for double hypernuclei production through the (K^-, K^+) reaction on a diamond target.

[9] S. Aoki et. al., to be published in Phys. Lett. B

[10] S. Aoki et. al., Prog. Theor. Phys. 85, (1991) 1287. ; K. Imai, Nucl. Phys. A547 (1992) 199c.

[11] G. Burgun et. al., Nucl. Phys. B8, (1968) 447. ; Dauber et. al., Phys. Rev. 179, (1969) 1262. ; A. De Bellefon et al., Nouv. Cimen. 7A,(1972) 567. ; Berthon et. al., Nouv. Cimen. 21A, (1974) 146. ; C. Baltay et. al., Phys. Rev. D9, (1974) 49.

[12] P.Beilliere et. al., Phys. Lett. B39, (1972) 671 ; G. Wilquet et. al., Phys. Lett. B57, (1975) 97.

[13] T. Iijima et. al., Nucl. Phys. A546, (1992) 588.

[14] C. Gobbi, C. B. Dover, A. Gal, Phys. Rev. C 50, (1994) 1594.

[15] Y.Nara, A.Ohnishi, T.Harada, A.Engel, Nucl. Phys. A in print.

[16] J.K. Ahn et. al., Nouv. Cimen. 107A, (1994) 2415.

[17] J.K. Ahn et. al., Nucl. Phys. A547, (1992) 211c.

[18] S. Yamashita, Ph.D. thesis, Kyoto University, KUNS 1332, (1995) (unpublished).

[19] Y. Itow, Ph.D. thesis, Kyoto University, KUNS 1362, (1995) (unpublished).

[20] Y. Itow et al., to be published.

[21] V.Flaminio, W.G.Moorhead, D.R.O.Morrison,N.Rivoire, Compilation of Cross-Sections II: K^+ and K^- Induced Reactions, CERN-HERA 83-02 (1983).

[22] The differential cross section for the $K^-p \rightarrow K^+\Xi^-$ process was parametrized to be $d\sigma/d\Omega_L = 0.66\epsilon^{+4.03\cos\theta}$ at the angular interval of $0.8 \leq \cos\theta_L \leq 1.0$.

[23] M.S. Chung, Ph.D. thesis, Korea University, (1995) (unpublished).

[24] Particle Date Group, Phys. Rev. D 54, (1996) 1.

[25] M. Iida, M.Sc. thesis, Aichi University of Education, (1996) (unpublished).

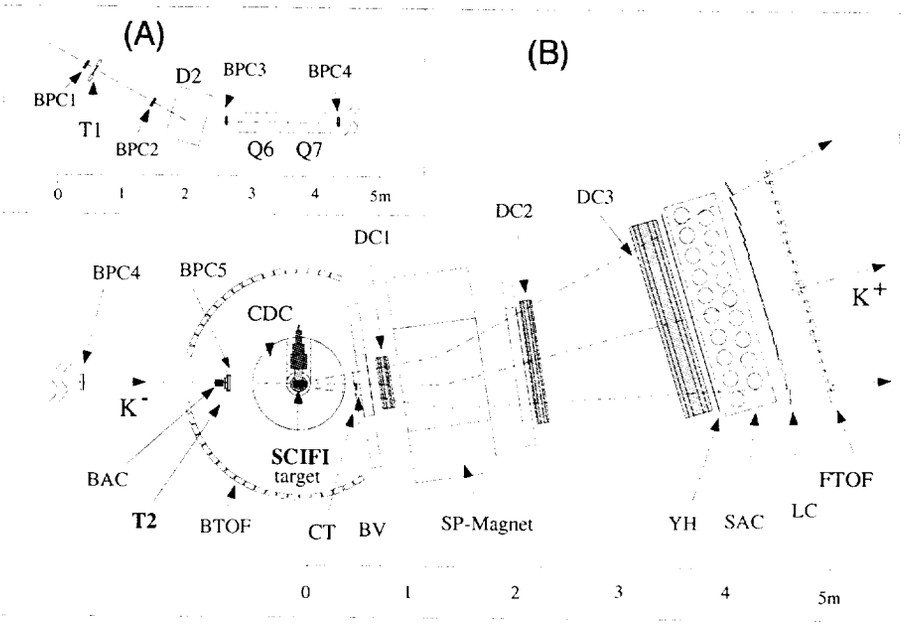

Figure 1: Experimental setup; (A) Beam line elements and detectors upstream of the target. (B) SCIFI target and K^+ tagging spectrometer

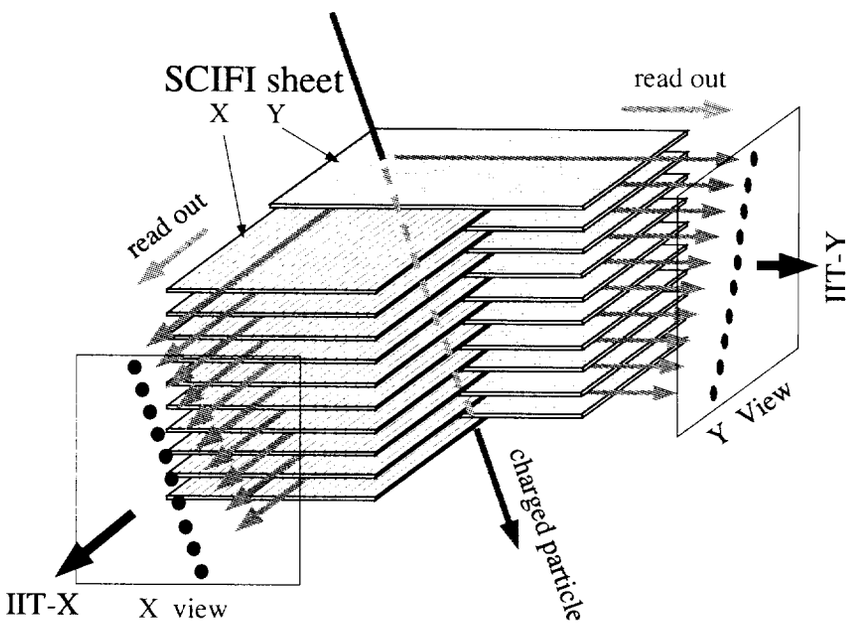

Figure 2: Schematic view of the SCIFI target

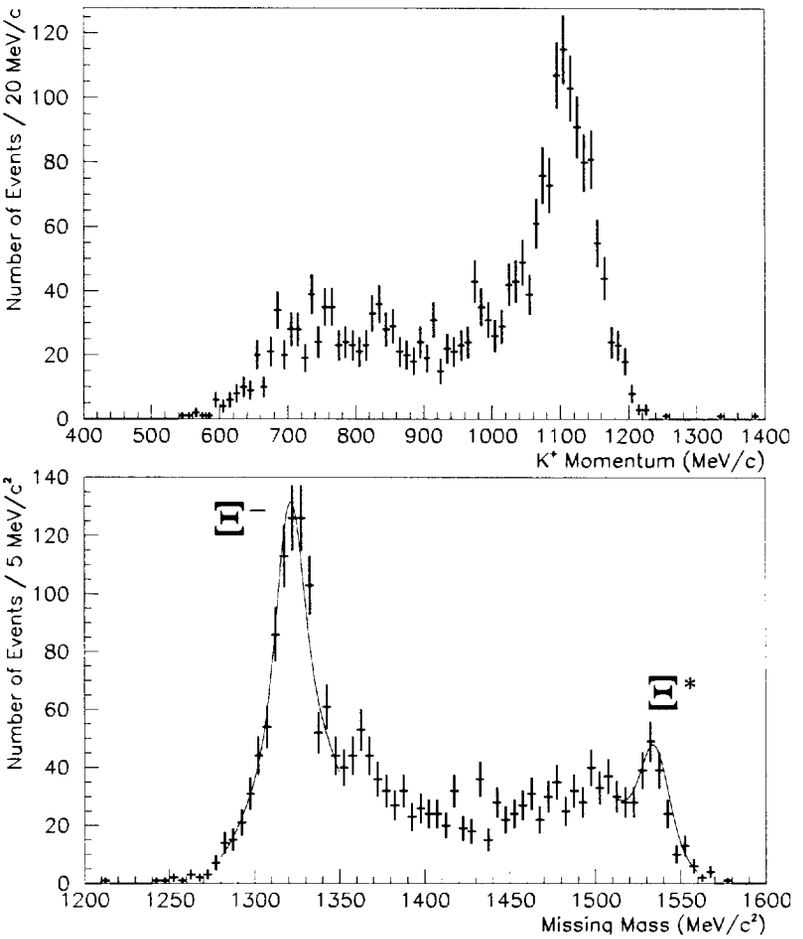

Figure 3: K^+ momentum spectrum (top) and missing mass spectrum(bottom). A proton target was assumed to calculate missing mass.

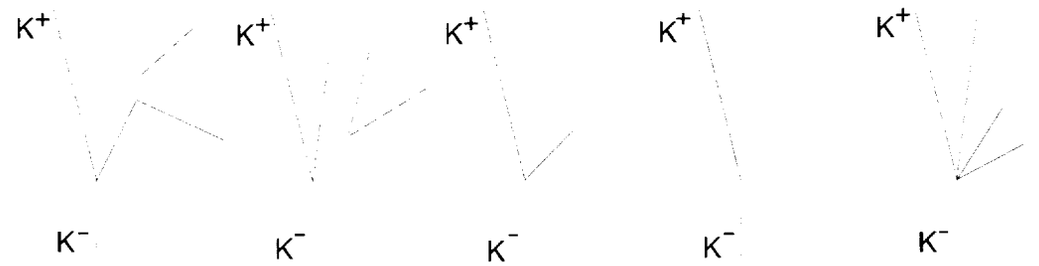

(a) D(DV)-type (b)Y(YV)-type (c) I-type (d) K-type (e) X-type

Figure 4: Event topologies of (K^-, K^+) reactions.

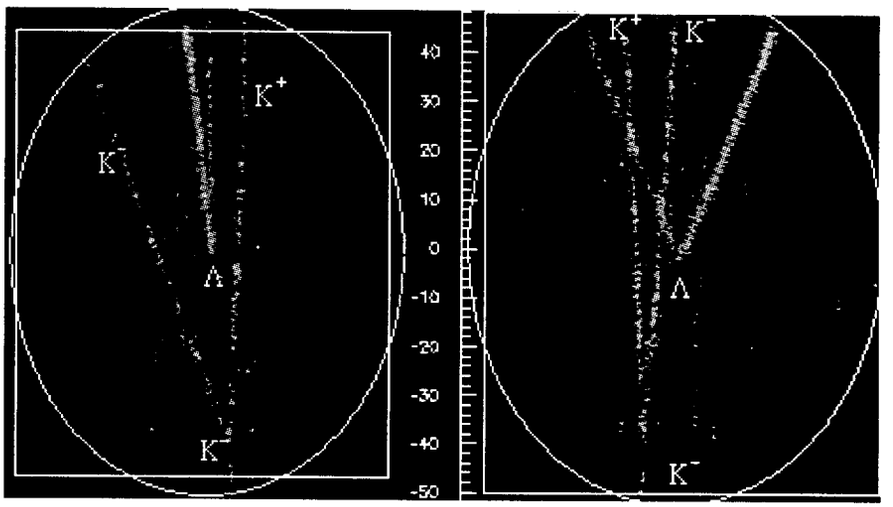

Figure 5: Typical event of scalar and vector meson production. The K^-K^+ pair and Λ decay are clearly seen in both XZ and YZ directions (Z is the beam direction).

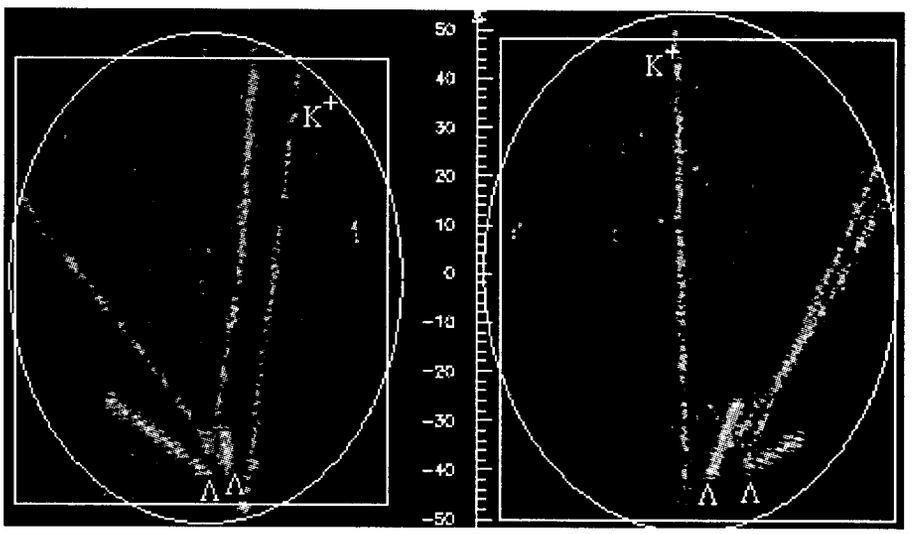

Figure 6: Typical $\Lambda\Lambda$ production event. Two Λ decays are clearly seen in the bottom of the figure.

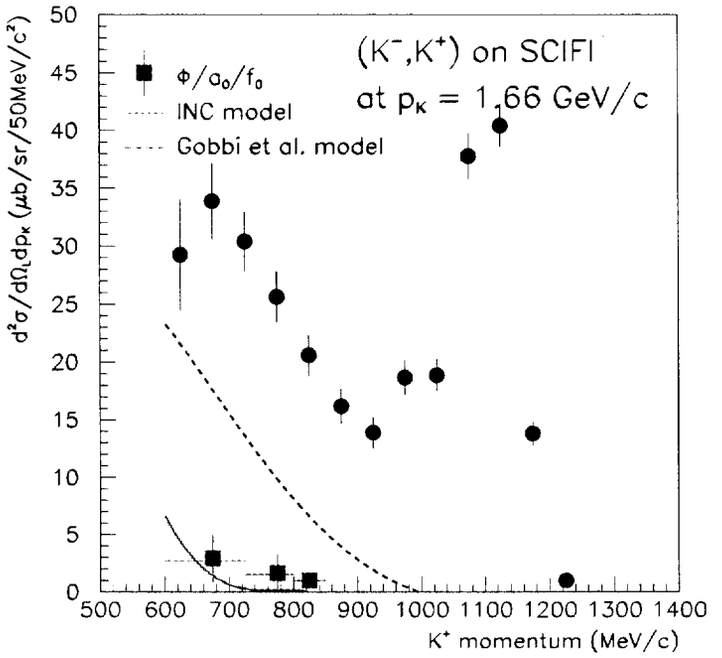

Figure 7: The double differential cross sections of (K^-, K^+) reactions (circle) and the sub-threshold $f_0/a_0/\phi$ meson productions followed by decaying into K^-K^+(square). The solid line indicates the intra-nuclear-cascade model calculation, while the dashed line shows the Gobbi et al.'s calculation[15].

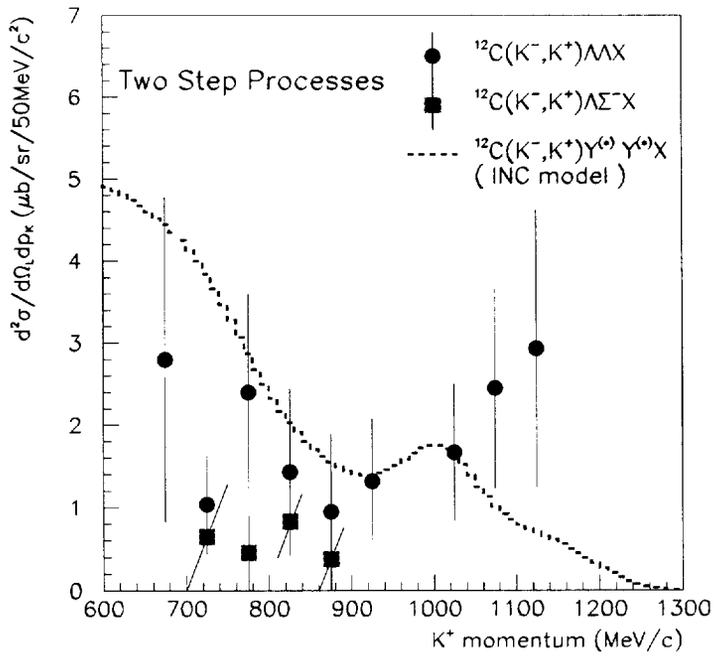

Figure 8: The double differential cross sections of two step processes. The closed circles indicate the $^{12}C(K^-, K^+)\Lambda\Lambda X$ reaction, while the squares represent the $^{12}C(K^-, K^+)\Lambda\Sigma^- X$ reaction. The dashed line shows the INC calculation on the total contribution of $^{12}C(K^-, K^+)Y^{(*)}Y^{(*)}X$ two-step processes.

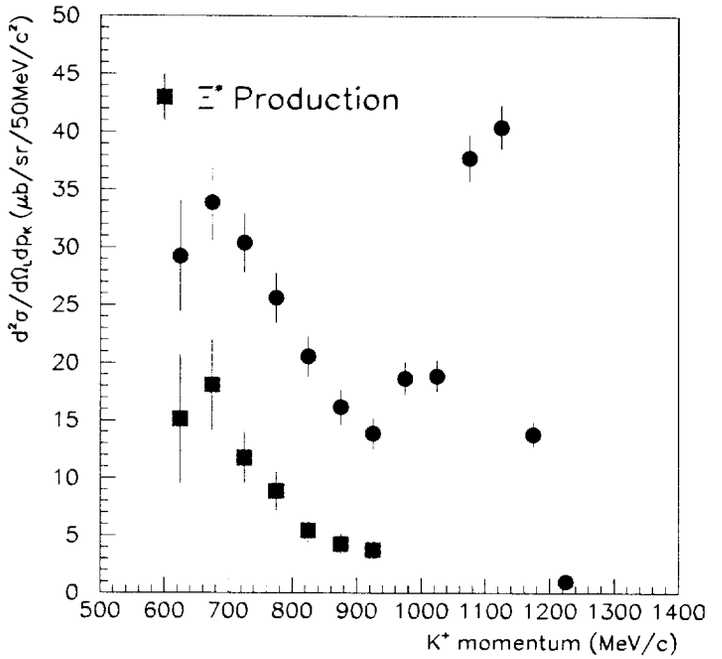

Figure 9: The double differential cross sections of (K^-, K^+) reaction(circle) and Ξ^* production followed by $\Xi^* \rightarrow \Xi\pi$ on the SCIFI target(square).

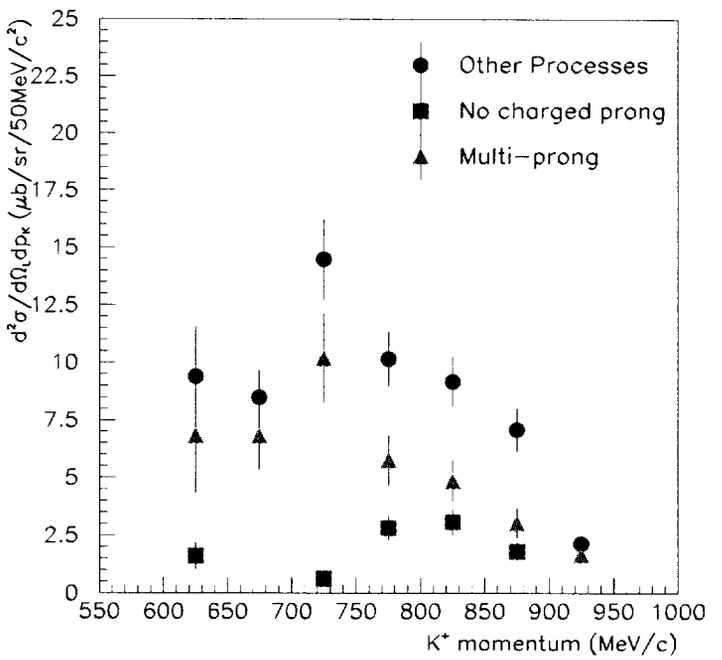

Figure 10: The double differential cross sections of other processes (circle) which were not identified for the scalar and vector meson productions, the two-step processes nor quasifree Ξ^-/Ξ^* productions. The multi-prong events(triangle) and no charged prong events(square) of other processes are shown.